Australian Government
Department of Defence
Science and Technology

Refinement of Out of Circularity and Thickness Measurements of a Cylinder for Finite Element Analysis

B.P. Phelps

Maritime Division
Defence Science and Technology Group

DST-Group-TN-1521

ABSTRACT

The as-built out-of-circularity (OOC) deviations from a perfectly round shape and plate thickness variations of a cylinder that is subjected to external pressure are known to have a significant effect on the collapse strength and must be accurately represented in finite element analysis to obtain accurate results. Often it is necessary to interpolate measurements from a relatively coarse grid to a refined finite element model and methods that have wide general acceptance are Fourier series and bi-linear interpolation. These methods have been implemented in an Excel spreadsheet to produce node and element data that can be used directly in the Strand7 finite element package, but the methods employed are suitable for other software as well.

Published by

Maritime Division
Defence Science and Technology Group
506 Lorimer St
Fishermans Bend, Victoria 3207 Australia

Telephone: 1300 333 362
Fax: (03) 9626 7999

AR-016-603
September 2016

APPROVED FOR PUBLIC RELEASE

Refinement of Out of Circularity and Thickness Measurements of a Cylinder for Finite Element Analysis

Executive Summary

The as-built out-of-circularity (OOC) deviations from a perfectly round shape and plate thickness variations of a cylinder that is subjected to external pressure are known to have a significant effect on the collapse strength. Non-linear finite element analysis (NL FEA) may be used to predict the collapse strength but the true shape and plate thickness of the cylinder must be modelled before it can be expected to obtain accurate results.

Often the OOC and plate thickness are measured only at discrete grid points on the cylinder surface so suitable methods of interpolation between these measured points are needed for model refinement so that modelling accuracy is maintained. Proven methods that have wide general acceptance are Fourier series and bi-linear interpolation and these methods have been implemented via an Excel spreadsheet to produce node and element data that can be used directly in the Strand7 finite element package through the inbuilt 'Online Editor' facility.

The methods employed are also suitable for other finite element software and a test case is used to demonstrate that the spreadsheet implementation provides accurate interpolation between measured data points.

This page is intentionally blank

Contents

This page is intentionally blank

1. Introduction

The as-built out-of-circularity (OOC) deviations from a perfectly round shape and plate thickness variations of a cylinder subjected to external pressure are known to have a significant effect on the collapse strength. When using non-linear finite element analysis (NL FEA) to model collapse behaviour, it is very important to ensure that the finite element model (FEM) accurately represents the true shape and plate thickness of the cylinder before it can be expected to obtain accurate results. Often OOC and plate thickness are measured only at discrete grid points on the cylinder surface so suitable methods of interpolation between these measured points is needed for model refinement so that modelling accuracy is maintained.

Plate thickness variations are usually within relatively small ranges and do not vary rapidly, so a simple bi-linear interpolation between the measured points is usually sufficient. A well-established method to interpolate the shape of a cylinder cross section from measurements of the radius at uniformly spaced angular positions was provided by Kendrick (1977) and is based on the Fourier theorem that periodic functions may be approximated through the superposition of sine and cosine functions. This paper outlines the approach taken to implementing these two methods in a Microsoft Excel spreadsheet to generate a refined grid of node coordinates and plate thickness values and gives examples of results obtained.

2. General Method

The general method of both the bi-linear and Fourier series interpolation methods is first outlined and then a test case example is provided to demonstrate the successful implementation of these methods through the Excel spreadsheet.

2.1 Plate thickness interpolation

For the bi-linear interpolation of plate thickness values it is assumed that the plate thickness is measured at specific points on a regularly spaced grid (both circumferentially and longitudinally) and that the FEM elements are refined only within the bounds of the rectangular shape defined by four adjacent grid points. The grid refinement is carried out in an integer number of uniform increments in both direction (although not necessarily the same for each directions) and the value of plate thickness of each element is interpolated from the measured values based on the relative position of the centroid of the refined grid element. The bi-linear interpolation method is applied between the four measurements points surrounding each element centroid as depicted in Figure 1.

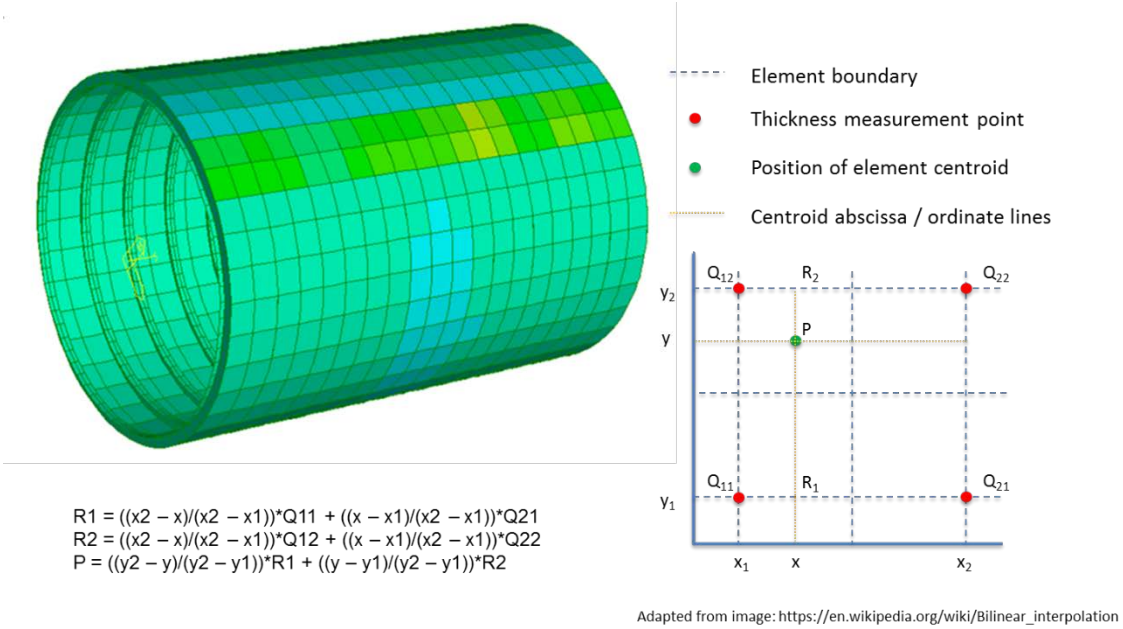

Figure 1. Depiction of bi-linear thickness interpolation method and indicative element thickness map

The thickness values measured at the four grid points (x_1, y_1), (x_1, y_2), (x_2, y_1) and (x_2, y_2) are designated as Q_{11}, Q_{12}, Q_{21} and Q_{22} respectively. Point **P** is the position of the element centroid and R_1 and R_2 are intermediate weighting values used in the calculation as shown in Figure *1*. As the centroid of the finite elements can never be coincident with a thickness measurement point, element thickness values will always be less than the maximum and greater than the minimum measured values, but never equal. The interpolation of element thickness therefore involves a certain degree of error that reduces as the element size is reduced.

2.2 OOC interpolation

The OOC of a cylinder is the deviation of the actual shape at a cross section from the mean circle and Kendrick (1970) suggested that the OOC of pressure vessels can be considered as composed of a combination of buckling mode shapes obtained by Fourier analysis of the two-dimensional pattern of shape deviations from a true cylinder. A method based on this approach for the analysis of chord gauge reading was described by Kendrick (1977) and is the basis of the method implemented in the Excel spreadsheet demonstrated with the test case below. The method proposes that the radius around the circumference of a cylinder at a particular section can be defined by the Fourier series summation:

$$\boldsymbol{R}(\emptyset) = \boldsymbol{b_0} + \boldsymbol{a_1}\sin(\boldsymbol{r}\emptyset) + \boldsymbol{b_1}\cos(\boldsymbol{r}\emptyset) + \sum_{\boldsymbol{n=2}}^{\infty} \boldsymbol{a_n}\sin(\boldsymbol{rn}\emptyset) + \boldsymbol{b_n}\cos(\boldsymbol{rn}\emptyset) \quad (1)$$

$$for\ \boldsymbol{r} = 0, 1, 2, \ldots . \boldsymbol{N} - 1.$$

where:

$\boldsymbol{N = N_{\emptyset}}$ is the number of evenly spaced radial measurements $\boldsymbol{R(\emptyset)}$ around the circumference,

$\boldsymbol{\emptyset = 2\pi/N_{\emptyset}}$ is the angular separation of measurements,

$\boldsymbol{b_0 = \frac{1}{N}\sum_{r=0}^{N-1} R_r}$ is the average radius,

$\boldsymbol{a_1 = \frac{2}{N}\sum_{r=0}^{N-1} R_r \sin(r\emptyset)}$ and $\boldsymbol{b_1 = \frac{2}{N}\sum_{r=0}^{N-1} R_r \cos(r\emptyset)}$

provide the offset of the true centre of the measurements from the nominal centre, and

$\boldsymbol{a_n = \frac{2}{N}\sum_{r=0}^{N-1} R_r \sin(rn\emptyset)}$ and $\boldsymbol{b_n = \frac{2}{N}\sum_{r=0}^{N-1} R_r \cos(rn\emptyset)}$

are the Fourier coefficients for a particular circumferential wave number, **n**.

Application of the Fourier theorem requires that the initial function $\boldsymbol{R(\emptyset)}$ be periodic.

2.3 Method of OOC refinement

Traditionally, measurements of the OOC of the pressure hull have been based on chord gauge measurements that are carried out at regular intervals along the pressure hull, and so as noted by MacKay (2007) it is often simpler to consider the OOC at discrete axial locations and to make use of a one-dimensional Fourier series to characterise the shape at each section. As the circumferential and longitudinal measurements are orthogonal, it is acceptable generally to use the one-dimensional Fourier series to refine the grid in each of the circumferential and the longitudinal directions in turn; however some manipulation of the measurement data is needed.

2.3.1 Assumptions and approximations

There are some inherent assumptions and approximations in the approach used that need to be highlighted as they do lead to some degree of error being generated. Key assumptions and approximations include:

i. Measurements are assumed to be on a regular, orthogonal, cylindrical coordinate grid that is evenly spaced in both the circumferential and longitudinal directions, although the spacing on one direction is not necessarily the same as in the other direction;
ii. It is common nowadays for OOC measurements to be carried out using photogrammetry or laser measurement methods that are referenced to a fixed origin rather than each section being measured independently as with chord gauge measurements. It is assumed therefore that radial values given for individual sections are relative to the nominal centreline axis and that perturbations of the true centre of each section relative to the axis are in fact real;
iii. The number of component sine/cosine waves (modes) that can be used in the summation in Equation (2) is limited to no more than half the number of data points around a circumference or along a meridian, as at least two points are required to define each wave component [MacKay (2007)].

2.3.2 Circumferential refinement

Refinement is carried out first in the circumferential direction at each measurement cross-section. The requirement that the measured radius $\boldsymbol{R}(\emptyset)$ around the circumference is periodic is satisfied at any particular section to the level of accuracy afforded by the closeness of the angular measurements. So to refine the grid in the circumferential direction, the Fourier coefficients for each measured section are calculated from the $\boldsymbol{N}_{\emptyset}$ measured circularity values and then the refined radial grid may be obtained by generating the Fourier sum for each new angular increment:

$$\boldsymbol{R}(\boldsymbol{\theta_s}) = \boldsymbol{b_0} + \sum_{n=1}^{\leq N/2} \boldsymbol{a_n} \sin(\boldsymbol{n\theta_s}) + \boldsymbol{b_k} \cos(\boldsymbol{n\theta_s}) \quad (2)$$

for $\boldsymbol{s} = 0, 1, 2, \ldots . \boldsymbol{M} - 1$.

where:

$\boldsymbol{M}$ is the number of evenly spaced radial values in the refined grid of the section, and

$$\boldsymbol{\theta_s} = \boldsymbol{s}.\boldsymbol{2\pi/M}$$

In the original theory outlined by Kendrick (1977), the summation in equation (2) was carried out from **n**=2 rather than **n**=1 as shown here. As noted above, $\boldsymbol{a_1}$ and $\boldsymbol{b_1}$ are the offsets of the true centre of the measurements from the nominal centre and so these values were excluded from the summation as the theory was applied to chord gauge measurements to obtain the OOC as a deviation from the true circle. There was no need to maintain the offset as the discussion was in regards to individual sections only and to demonstrate that the refined grid reproduced the correct OOC relative to the true centre. For FEM applications however, if the true shape of a cylinder is to be maintained when the grid refinement is carried out, then the terms $\boldsymbol{a_1}$ and $\boldsymbol{b_1}$ must be included so that the position of the true centre of each section relative to the centreline axis of the cylinder is maintained. If these terms are not included then each of the reformed grid sections would have their centre shifted to the centreline axis, thereby distorting the reconstructed shape from the measured shape. The summation in Equation (2) is therefore commenced at **n**=1 and the effect is demonstrated by way of an example in the 'Test Case' given in Section 3.

2.3.3 Longitudinal refinement

To refine the grid in the longitudinal direction, the same process is carried out using the calculated $\boldsymbol{R}(\boldsymbol{\theta_s})$ values along the meridian for each angular step, rather than around the circumference at each station. As noted above, application of the Fourier theorem requires that the initial function $\boldsymbol{R}(\boldsymbol{\theta_s})$ be periodic, but this is not generally true along the meridians. It is therefore necessary to manipulate the data so that this requirement may be satisfied by reflecting the radial values along each meridian about one end to generate a pseudo periodic function along the meridian. This approach also has the advantage that it effectively doubles the number of data points used to calculate the Fourier coefficients and the number of longitudinal modes available for reconstruction of the refined shape using Equation (2). Only the first half of the refined data set is needed otherwise it is also reflected about the end.

2.3.4 Spreadsheet implementation

Radial measurements are provided in an Excel spreadsheet table of $N_{\emptyset}$ rows by N_s columns, where $N_{\emptyset}$ is the number of angular measurements and N_s is the number of measurement stations. The grid is to be refined into N_θ by N_r circumferential and longitudinal values respectively. The main steps involved are as follows:

i. Read the $N_{\emptyset}$ by N_s tabular values.
ii. Calculate the $N_{\emptyset}$ Fourier coefficients b_0, a_1, b_1, a_n and b_n for each station; Equation (1),
iii. Use the Fourier sum to calculate the N_θ radial values of the refined grid around the circumference at each of the N_s stations; Equation (2),
iv. Reflect the N_s radial values for each of the N_θ meridians about the end away from the origin,
v. Using the **2 *** N_s values for each meridian, calculate a new set of Fourier coefficients b_0', a_1', b_1', a_n' and b_n',
vi. Reapply the Fourier sum Equation (2) with the new coefficients to calculate the N_r refined grid values along each of the N_θ meridians,

The grid is now refined in both directions, giving N_θ by N_r radial values.

3. Test Case

The method outlined above has been implemented through an Excel VBA spread sheet to generate nodal coordinate values of the refined grid together with plate element definitions in a form that may be pasted directly into a Strand7® model using the inbuilt 'Online Editor' facility. The Excel spreadsheet reads the tables of radial and thickness measurements and a refined grid is produced based on user specified levels of subdivision in both the circumferential and longitudinal directions. This enables models to be developed very quickly and consistently, for example the node sequence definitions are the same for all plate elements and so element normals are always in the same directions. The results of a test case example are given below to demonstrate the grid refinement using the Excel spreadsheet.

3.1.1 Plate thickness mapping

Plate thickness measurements for the test case are given in Table 1 and a contour map of the thickness distribution of a refined finite element model is given in Figure 2. Cells are colour shaded to highlight different thickness ranges so that they may be visually compared to the thickness contour map obtained from the Strand7 software. The matching of colours between the table and the contour map is only approximately similar because Table 1 gives thickness at the corner nodes whilst on the contour map colour represents the thickness at the centroid. Additionally different software is used and ranges and colour pallets do not match exactly; nevertheless similarity in the distribution patterns is evident.

Table 1. Plate thickness measurements for test case.

Station No.:		2	4	6	8	10	12	14	16	18	20
Long. Position		80	240	400	560	720	880	1040	1200	1360	1520
CIRCUMFERENTIAL LOCATION (degrees)	10	6.76	6.79	6.74	6.86	6.79	6.82	6.83	6.78	6.85	6.83
	20	6.79	6.79	6.81	6.86	6.75	6.74	6.81	6.8	6.86	6.74
	30	6.77	6.74	6.72	6.75	6.53	6.69	6.89	6.82	6.71	6.72
	40	6.8	6.8	6.79	6.79	6.42	6.7	6.81	6.9	6.74	6.72
	50	6.82	6.79	6.78	6.8	6.43	6.78	6.78	6.8	6.69	6.74
	60	6.86	6.81	6.77	6.82	6.52	6.58	6.78	6.72	6.74	6.86
	70	6.83	6.78	6.78	6.8	6.49	6.59	6.81	6.8	6.72	6.71
	80	6.83	6.86	6.82	6.88	6.5	6.71	6.8	6.77	6.75	6.71
	90	6.93	6.85	6.79	6.89	6.37	6.62	6.78	6.75	6.71	6.69
	100	6.86	6.86	6.85	6.82	6.68	6.72	6.8	6.78	6.72	6.68
	110	6.87	6.83	6.81	6.85	6.79	6.78	6.78	6.79	6.77	6.72
	120	6.82	6.84	6.82	6.89	6.81	6.73	6.85	6.81	6.72	6.72
	130	6.84	6.84	6.79	6.85	6.85	6.73	6.82	6.81	6.72	6.74
	140	6.85	6.86	6.87	6.84	6.75	6.74	6.77	6.77	6.81	6.83
	150	6.84	6.82	6.95	6.85	6.78	6.77	6.78	6.8	6.79	6.75
	160	6.8	6.82	6.78	6.83	6.82	6.75	6.81	6.81	6.79	6.78
	170	6.81	6.79	6.8	6.88	6.89	6.8	6.8	6.79	6.82	6.84
	180	6.81	6.87	6.83	6.83	6.73	6.85	6.82	6.75	6.72	6.79
	190	6.81	6.85	6.84	6.83	6.74	6.82	6.8	6.93	6.76	6.74
	200	6.82	6.87	6.82	6.83	6.82	6.84	6.81	6.75	6.72	6.74
	210	6.86	6.85	6.82	6.84	6.82	6.88	6.84	6.83	6.72	6.76
	220	6.84	6.83	6.86	6.92	6.8	6.8	6.82	6.79	6.75	6.77
	230	6.93	6.88	6.85	6.88	6.79	6.8	6.79	6.82	6.82	6.77
	240	6.85	6.85	6.87	6.82	6.8	6.79	6.79	6.77	6.73	6.75
	250	6.95	6.92	6.86	6.95	6.79	6.82	6.86	6.77	6.75	6.74
	260	6.94	6.96	6.88	6.94	6.83	6.86	6.87	6.83	6.82	6.78
	270	6.93	6.89	6.9	6.94	6.82	6.9	6.89	6.97	6.77	6.72
	280	6.87	6.87	6.92	6.85	6.84	6.85	6.74	6.87	6.81	6.72
	290	6.87	6.86	6.88	6.85	6.81	6.82	6.79	6.76	6.79	6.72
	300	6.82	6.82	6.78	6.89	6.83	6.83	6.79	6.77	6.73	6.72
	310	6.88	6.82	6.84	6.84	6.78	6.81	6.95	6.93	6.82	6.73
	320	6.87	6.77	6.89	6.87	6.78	6.85	6.85	6.89	6.83	6.76
	330	6.86	6.83	6.81	6.89	6.79	6.86	6.84	6.83	6.76	6.79
	340	6.46	6.51	6.49	6.48	6.39	6.45	6.58	6.57	6.48	6.45
	350	6.54	6.5	6.69	6.41	6.47	6.43	6.56	6.44	6.38	6.33
	360	8.54	8.96	7.35	9.25	9.27	9.76	11.2	8.4	10.38	9.01
	Longitudinal seam weld is a theta = 0/360 deg										

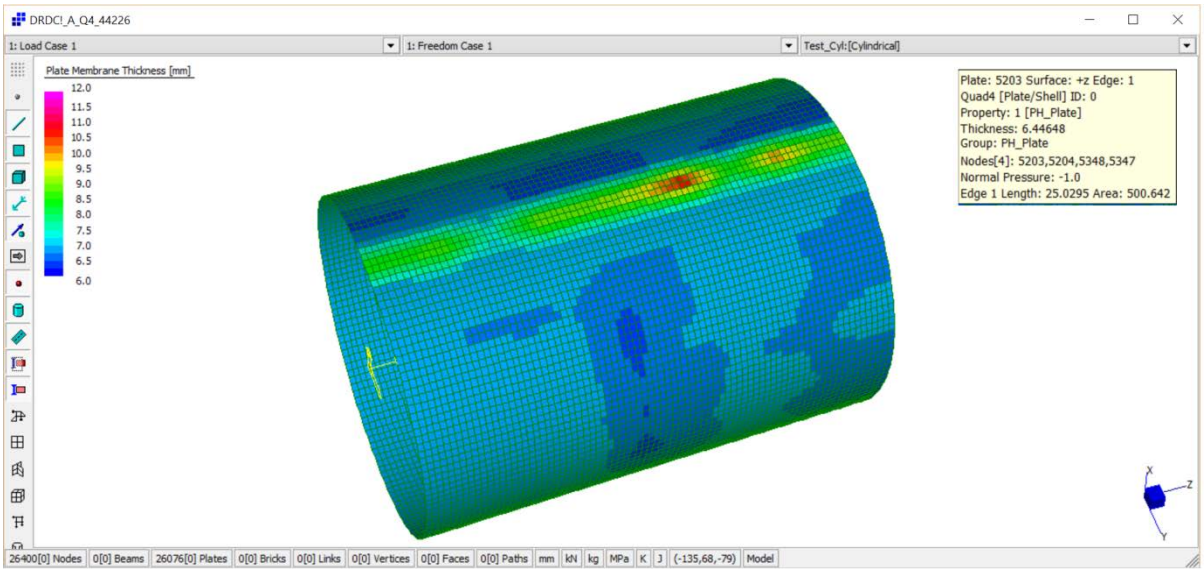

Figure 2. Example of thickness distribution in the refined finite element model. Note that the longitudinal seam weld at θ = 0° (= 360°) runs along the green area and through the centre of the red coloured elements.

As mentioned previously, the element thickness values always lie somewhere between the maximum and minimum of the four measured values used in the interpolation, so there is no direct comparison of measured-to-calculated values. Separate hand calculations for several different grid locations have been conducted to verify the thickness values calculated by the spreadsheet and all have been in agreement. For example, plate element 5203 of the model shown in Figure 2 has its centroid located at a radial angle of $\boldsymbol{\theta}$ = 46.2503° and a longitudinal position of $\mathbf{Z}$ = 730 mm, which is located within the four grid points highlighted by the heavy border in Table 1. Using the equations shown in Figure *1* it is relatively easy to confirm the thickness value of 6.44648 mm as shown in Figure 2.

The thickness measurements in Table 1 correspond to mid-bay positions between cylinder ring stiffeners and so do not extend to the ends of the cylinder where frames are located in this example. Interpolation of plate thickness through the first and last half-bay sections of shell plating is then based only on the two nearest measured values.

3.1.2 OOC comparisons

To demonstrate that the spreadsheet reliably reproduces the original radial values in the refined grid a 'refined' model based on measurement values given in Table 1 is produced via the spreadsheet to the same grid as the original measurements (i.e. there is no actual refinement and so $\boldsymbol{N_\theta = N_\emptyset}$ and $\boldsymbol{N_r = N_s}$). The resulting grid is given in Table 3; it should be noted that that 0° in Table 3 corresponds to 360° in Table 2.

Direct comparison of measured and calculated values provides the following analysis of the differences with the following statistical results:

Average error for all values:	5.38358E-14	mm
Standard deviation for all values:	0.016269599	mm
Maximum +ve error value:	0.034910197	mm
Minimum -ve error value:	-0.0349102	mm

The standard deviation error is approximately only two thirds of the quoted accuracy for the system used to make the measurements so is considered within acceptable levels.

The results from a further example where the grid is actually refined by subdividing twice in both directions is shown for two sections in Figure 3. Section 1 is the first measurement station and Section 11 is at the middle of the cylinder. The cylinder shell was formed from a single steel plate and the pulling-in of the plating at the longitudinal weld seam at 0° is clearly evident. Inspection of similar graphs for all sections indicates similarly good comparison between the measured and calculated values in all cases.

Table 2. Test case radial measurements (to first significant figure only, maximum and minimum values highlighted by heavy borders)

Station No.:	1	2	3	4	5	6	7	8	9	10	11	12	13	14	15	16	17	18	19	20	21
Angle:																					
10	572.28	572.06	572.28	572.11	573.10	572.30	572.83	572.76	573.35	572.67	572.84	572.42	572.52	572.31	572.49	571.77	571.74	571.54	571.68	571.66	572.53
20	573.29	573.31	573.23	573.25	573.50	573.55	573.78	573.89	574.33	574.12	574.19	574.15	574.31	574.15	574.17	573.76	573.50	573.58	573.57	573.76	574.01
30	574.32	574.43	574.67	574.60	575.19	574.84	575.11	575.11	575.57	575.26	575.30	575.29	575.62	575.40	575.61	575.33	575.36	575.24	575.28	575.29	575.62
40	575.71	575.82	576.01	576.23	576.64	576.36	576.68	576.26	576.30	576.27	576.53	576.47	576.67	576.51	576.69	576.64	576.95	576.83	577.06	576.88	576.98
50	576.72	576.86	577.04	577.29	577.77	577.36	577.45	577.27	577.62	577.56	578.06	577.89	578.13	577.86	577.83	577.90	578.07	578.00	578.20	578.25	578.30
60	577.93	578.08	577.97	577.99	578.35	578.31	578.42	578.50	579.03	578.80	578.82	578.77	579.04	578.89	579.12	579.01	578.85	578.88	578.92	578.99	579.03
70	578.28	578.34	578.36	578.43	578.89	578.91	579.22	579.03	579.44	578.98	579.08	578.99	579.16	579.05	579.18	579.18	579.39	579.26	579.22	579.20	579.31
80	578.48	578.48	578.48	578.48	578.97	578.56	578.67	578.62	579.10	578.69	578.79	578.76	578.81	578.65	578.64	578.49	578.45	578.49	578.60	578.67	578.80
90	577.68	577.65	577.63	577.49	577.63	577.40	577.66	577.60	578.15	577.90	578.10	577.98	577.96	577.78	577.72	577.62	577.41	577.39	577.47	577.49	577.57
100	576.77	576.75	576.66	576.50	576.72	576.53	576.91	576.58	576.99	576.70	576.91	576.81	576.96	576.68	576.94	576.72	576.73	576.62	576.53	576.51	576.56
110	575.83	575.83	575.81	575.70	575.91	575.86	576.07	575.61	575.93	575.63	575.93	575.71	575.84	575.65	575.58	575.57	575.61	575.74	575.70	575.77	575.88
120	575.14	575.14	575.06	575.05	575.39	574.99	575.13	574.81	575.06	574.75	575.04	574.90	575.24	575.11	575.17	575.08	575.04	575.20	575.30	575.37	575.44
130	574.42	574.50	574.48	574.31	574.35	574.13	574.41	574.18	574.55	574.16	574.44	574.26	574.66	574.66	574.72	574.74	574.71	574.95	574.98	575.13	575.19
140	573.87	574.00	573.98	573.68	573.81	573.67	574.13	573.85	574.04	573.80	574.19	574.07	574.34	574.33	574.45	574.48	574.48	574.71	574.73	574.92	575.08
150	573.46	573.66	573.81	573.61	573.89	573.91	574.05	573.69	573.75	573.62	574.21	574.01	574.19	574.17	574.16	574.19	574.23	574.47	574.38	574.60	574.84
160	573.55	573.70	573.76	573.82	574.17	573.93	574.15	573.92	574.00	573.94	574.39	574.08	574.23	574.12	574.04	574.04	574.04	574.08	574.01	574.24	574.40
170	573.64	573.73	573.75	573.85	574.16	573.93	574.35	574.25	574.58	574.25	574.46	574.12	574.28	574.08	573.97	573.96	573.81	573.86	573.78	573.80	573.88
180	573.79	573.89	573.90	573.86	574.16	573.79	574.13	574.04	574.01	574.02	574.32	574.16	574.30	573.94	573.82	573.82	573.91	573.88	573.72	573.74	573.65
190	574.34	574.18	573.87	573.96	574.56	574.19	574.24	574.21	574.23	574.21	574.53	574.31	574.55	574.25	574.07	573.91	574.05	573.91	573.98	573.94	573.90
200	575.13	575.01	575.05	574.63	574.97	574.82	575.13	574.92	574.83	574.79	575.01	574.73	574.79	574.73	574.57	574.46	574.65	574.38	574.44	574.43	574.50
210	575.15	575.49	575.62	575.30	575.62	575.31	575.63	575.32	575.26	575.25	575.51	575.24	575.21	575.17	575.15	575.17	575.19	575.02	575.04	574.97	574.90
220	575.86	576.04	576.04	575.89	576.34	575.82	575.99	575.83	575.92	575.71	576.02	575.63	575.63	575.70	575.81	575.84	575.82	575.70	575.78	575.66	575.55
230	576.69	576.52	576.32	576.27	576.78	576.20	576.29	576.16	576.28	576.05	576.16	576.07	576.33	576.14	576.14	576.13	576.27	576.22	576.40	576.33	576.29
240	576.26	576.52	576.44	576.48	576.98	576.52	576.67	576.36	576.46	576.18	576.30	576.28	576.34	576.30	576.32	576.43	576.61	576.62	576.88	576.95	577.09
250	576.33	576.50	576.70	576.82	577.25	576.87	577.06	576.85	576.99	576.69	576.98	576.75	576.74	576.68	576.68	576.71	576.77	576.96	577.28	577.33	577.43
260	576.39	576.72	576.90	576.83	577.14	577.02	577.44	577.27	577.59	577.17	577.45	577.24	577.42	577.35	577.46	577.31	577.22	577.29	577.55	577.59	577.56
270	576.26	576.57	576.64	576.67	577.16	576.92	577.19	577.17	577.59	577.16	577.58	577.48	577.68	577.67	577.85	577.90	578.12	577.95	578.04	578.08	578.19
280	576.02	576.19	576.25	576.25	576.87	576.70	577.10	576.82	577.40	577.22	578.07	577.88	578.10	577.97	578.14	578.30	578.48	578.46	578.63	578.75	578.65
290	576.68	576.51	576.55	576.27	576.59	576.44	576.81	576.79	577.39	577.07	577.63	577.67	578.15	578.08	578.35	578.30	578.30	578.35	578.59	578.50	578.33
300	576.66	576.67	576.78	576.77	577.22	576.88	577.12	577.07	577.61	577.04	577.45	577.26	577.64	577.69	577.94	577.84	577.68	577.65	577.82	577.67	577.36
310	576.60	576.68	576.69	576.82	577.35	576.88	576.85	576.81	577.20	576.72	577.24	576.73	576.85	576.83	577.02	577.06	577.34	577.17	577.22	577.02	576.67
320	576.14	576.25	576.39	576.10	576.64	576.20	576.58	576.15	576.38	575.82	576.50	576.03	576.07	575.99	576.06	575.87	575.85	575.87	575.85	575.72	575.39
330	575.00	575.14	575.36	575.02	575.73	575.03	575.20	574.97	575.23	574.74	575.27	574.86	575.10	574.69	574.63	574.32	574.22	574.10	573.99	574.15	574.16
340	574.06	574.12	574.10	573.87	574.49	573.94	574.28	573.94	574.42	573.88	574.19	573.31	573.20	573.04	573.18	573.01	572.87	572.79	572.95	573.15	573.64
350	572.93	572.67	572.63	571.97	572.71	572.14	572.81	572.45	573.21	572.34	572.59	571.57	571.74	571.41	571.66	571.25	571.31	570.88	571.40	571.27	572.07
360	571.25	571.16	571.45	571.10	571.76	571.28	571.40	572.64	572.67	572.43	571.66	571.77	571.17	571.34	570.90	570.44	570.38	569.77	570.09	569.91	570.39

Table 3. Spreadsheet output radial measurements (to two significant figures, maximum and minimum values highlighted by heavy borders)

Station No.:	1	2	3	4	5	6	7	8	9	10	11	12	13	14	15	16	17	18	19	20	21
Angle:																					
0	571.24	571.17	571.46	571.10	571.74	571.29	571.41	572.68	572.66	572.46	571.66	571.80	571.16	571.35	570.92	570.46	570.37	569.76	570.09	569.91	570.36
10	572.29	572.05	572.27	572.10	573.12	572.29	572.82	572.72	573.35	572.64	572.84	572.40	572.53	572.29	572.47	571.76	571.75	571.55	571.68	571.65	572.55
20	573.28	573.33	573.24	573.26	573.49	573.56	573.79	573.92	574.33	574.15	574.19	574.18	574.30	574.16	574.19	573.77	573.49	573.57	573.57	573.76	573.99
30	574.33	574.41	574.67	574.59	575.21	574.84	575.10	575.08	575.57	575.23	575.30	575.26	575.63	575.38	575.59	575.32	575.38	575.25	575.28	575.29	575.65
40	575.70	575.83	576.02	576.23	576.62	576.37	576.69	576.30	576.29	576.30	576.53	576.50	576.66	576.53	576.71	576.66	576.94	576.82	577.05	576.89	576.95
50	576.72	576.84	577.03	577.29	577.79	577.35	577.43	577.23	577.63	577.53	578.06	577.87	578.14	577.85	577.81	577.89	578.08	578.01	578.20	578.25	578.33
60	577.92	578.09	577.97	577.99	578.33	578.31	578.43	578.54	579.02	578.83	578.82	578.80	579.02	578.91	579.14	579.02	578.83	578.87	578.92	579.00	579.01
70	578.29	578.32	578.35	578.42	578.91	578.91	579.21	578.99	579.45	578.95	579.08	578.96	579.17	579.03	579.17	579.16	579.41	579.26	579.23	579.19	579.34
80	578.47	578.50	578.49	578.49	578.95	578.56	578.68	578.65	579.10	578.72	578.79	578.79	578.80	578.67	578.66	578.50	578.44	578.48	578.59	578.67	578.77
90	577.69	577.64	577.62	577.48	577.65	577.39	577.65	577.57	578.15	577.87	578.11	577.95	577.97	577.77	577.71	577.61	577.42	577.40	577.47	577.49	577.60
100	576.77	576.76	576.67	576.51	576.71	576.53	576.93	576.62	576.98	576.73	576.91	576.84	576.94	576.70	576.96	576.73	576.72	576.62	576.53	576.51	576.53
110	575.84	575.81	575.81	575.69	575.92	575.85	576.06	575.57	575.94	575.60	575.93	575.69	575.85	575.63	575.57	575.56	575.62	575.75	575.71	575.77	575.91
120	575.13	575.15	575.06	575.06	575.37	575.00	575.14	574.84	575.05	574.78	575.04	574.93	575.23	575.13	575.19	575.09	575.03	575.19	575.30	575.38	575.41
130	574.43	574.48	574.47	574.30	574.36	574.13	574.40	574.14	574.56	574.14	574.44	574.23	574.67	574.64	574.70	574.73	574.72	574.96	574.98	575.12	575.22
140	573.86	574.01	573.98	573.68	573.79	573.68	574.15	573.89	574.03	573.83	574.19	574.09	574.33	574.35	574.47	574.49	574.47	574.70	574.72	574.92	575.05
150	573.47	573.64	573.81	573.61	573.91	573.90	574.03	573.66	573.76	573.59	574.21	573.98	574.20	574.15	574.14	574.17	574.24	574.47	574.39	574.60	574.87
160	573.54	573.72	573.76	573.82	574.16	573.94	574.16	573.95	574.00	573.97	574.39	574.11	574.22	574.14	574.06	574.06	574.03	574.07	574.00	574.24	574.37
170	573.65	573.71	573.74	573.84	574.18	573.93	574.33	574.21	574.59	574.22	574.46	574.10	574.29	574.07	573.96	573.95	573.82	573.86	573.79	573.80	573.91
180	573.78	573.91	573.90	573.87	574.14	573.80	574.14	574.07	574.00	574.05	574.31	574.18	574.28	573.96	573.84	573.83	573.90	573.87	573.72	573.74	573.62
190	574.35	574.17	573.86	573.95	574.58	574.18	574.22	574.17	574.24	574.18	574.53	574.29	574.56	574.23	574.05	573.89	574.06	573.92	573.98	573.93	573.93
200	575.12	575.03	575.05	574.64	574.96	574.83	575.14	574.95	574.82	574.82	575.00	574.75	574.78	574.74	574.59	574.47	574.64	574.37	574.44	574.44	574.47
210	575.16	575.48	575.61	575.29	575.64	575.30	575.62	575.28	575.26	575.22	575.51	575.22	575.22	575.16	575.13	575.15	575.20	575.03	575.05	574.97	574.93
220	575.85	576.06	576.05	575.90	576.32	575.82	576.00	575.87	575.91	575.73	576.02	575.65	575.62	575.71	575.83	575.85	575.81	575.70	575.78	575.66	575.53
230	576.70	576.50	576.31	576.26	576.80	576.19	576.28	576.13	576.28	576.02	576.17	576.04	576.34	576.13	576.12	576.12	576.28	576.22	576.41	576.33	576.32
240	576.25	576.54	576.45	576.48	576.96	576.53	576.69	576.39	576.45	576.21	576.30	576.30	576.32	576.32	576.34	576.44	576.60	576.61	576.88	576.95	577.06
250	576.34	576.48	576.70	576.81	577.26	576.86	577.05	576.81	577.00	576.66	576.99	576.72	576.75	576.66	576.66	576.69	576.78	576.97	577.29	577.33	577.46
260	576.39	576.73	576.91	576.84	577.12	577.03	577.45	577.31	577.59	577.20	577.45	577.27	577.40	577.37	577.48	577.32	577.21	577.28	577.54	577.60	577.54
270	576.27	576.55	576.63	576.66	577.17	576.91	577.18	577.14	577.59	577.14	577.58	577.45	577.69	577.65	577.84	577.89	578.13	577.96	578.04	578.07	578.21
280	576.01	576.20	576.25	576.26	576.85	576.71	577.11	576.86	577.39	577.25	578.07	577.91	578.08	577.99	578.15	578.32	578.47	578.45	578.63	578.75	578.62
290	576.69	576.49	576.54	576.27	576.61	576.43	576.79	576.76	577.39	577.04	577.63	577.64	578.16	578.07	578.34	578.28	578.31	578.36	578.59	578.50	578.36
300	576.65	576.68	576.79	576.77	577.21	576.88	577.14	577.11	577.60	577.07	577.44	577.29	577.63	577.70	577.96	577.86	577.67	577.64	577.82	577.68	577.34
310	576.61	576.66	576.68	576.81	577.37	576.87	576.84	576.78	577.20	576.69	577.24	576.71	576.86	576.81	577.01	577.05	577.35	577.18	577.22	577.02	576.69
320	576.13	576.27	576.39	576.11	576.63	576.21	576.59	576.19	576.38	575.85	576.50	576.06	576.06	576.01	576.08	575.89	575.84	575.87	575.84	575.72	575.36
330	575.00	575.13	575.35	575.02	575.75	575.02	575.18	574.94	575.24	574.71	575.27	574.84	575.11	574.68	574.61	574.30	574.23	574.11	574.00	574.15	574.19
340	574.06	574.13	574.11	573.88	574.48	573.95	574.29	573.97	574.42	573.91	574.19	573.34	573.19	573.05	573.20	573.02	572.85	572.79	572.94	573.16	573.62
350	572.94	572.66	572.62	571.97	572.73	572.13	572.80	572.41	573.21	572.31	572.60	571.54	571.75	571.39	571.64	571.24	571.32	570.89	571.40	571.26	572.10

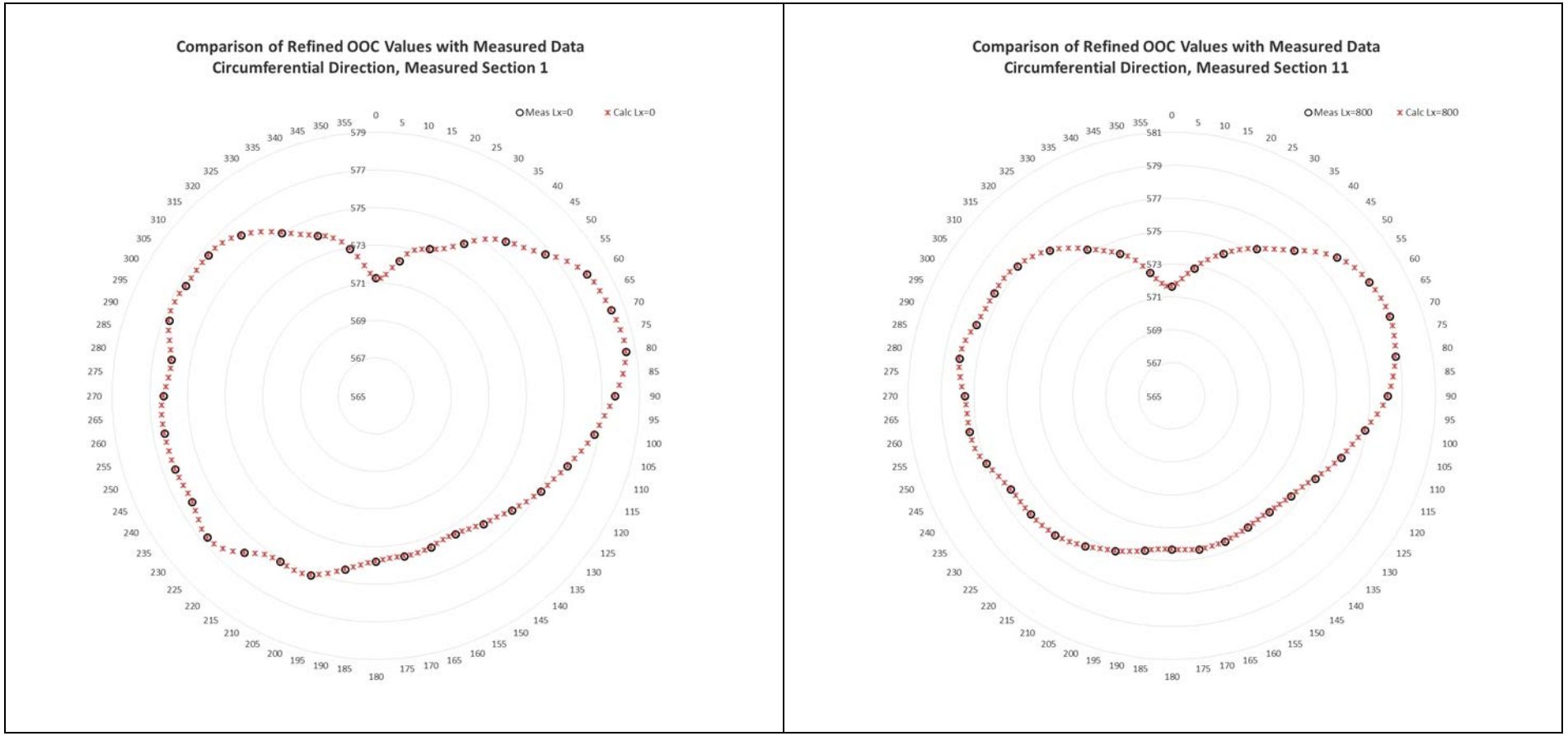

Figure 3. Comparison of measured (O) and calculated (×) radial values at two measurement sections. The range of radius axis values is restricted to exaggerate the variation from a mean radius of approximated 572 mm.

To check refinement in the longitudinal direction, Figure 4 shows a comparison of measured and calculated radius values along two meridians. The 'Radius' axis values are restricted to a small range to exaggerate variation from the mean radius and it can be seen that there is excellent correlation along the entire length. Inspection of other meridians has shown similarly good comparisons in all cases.

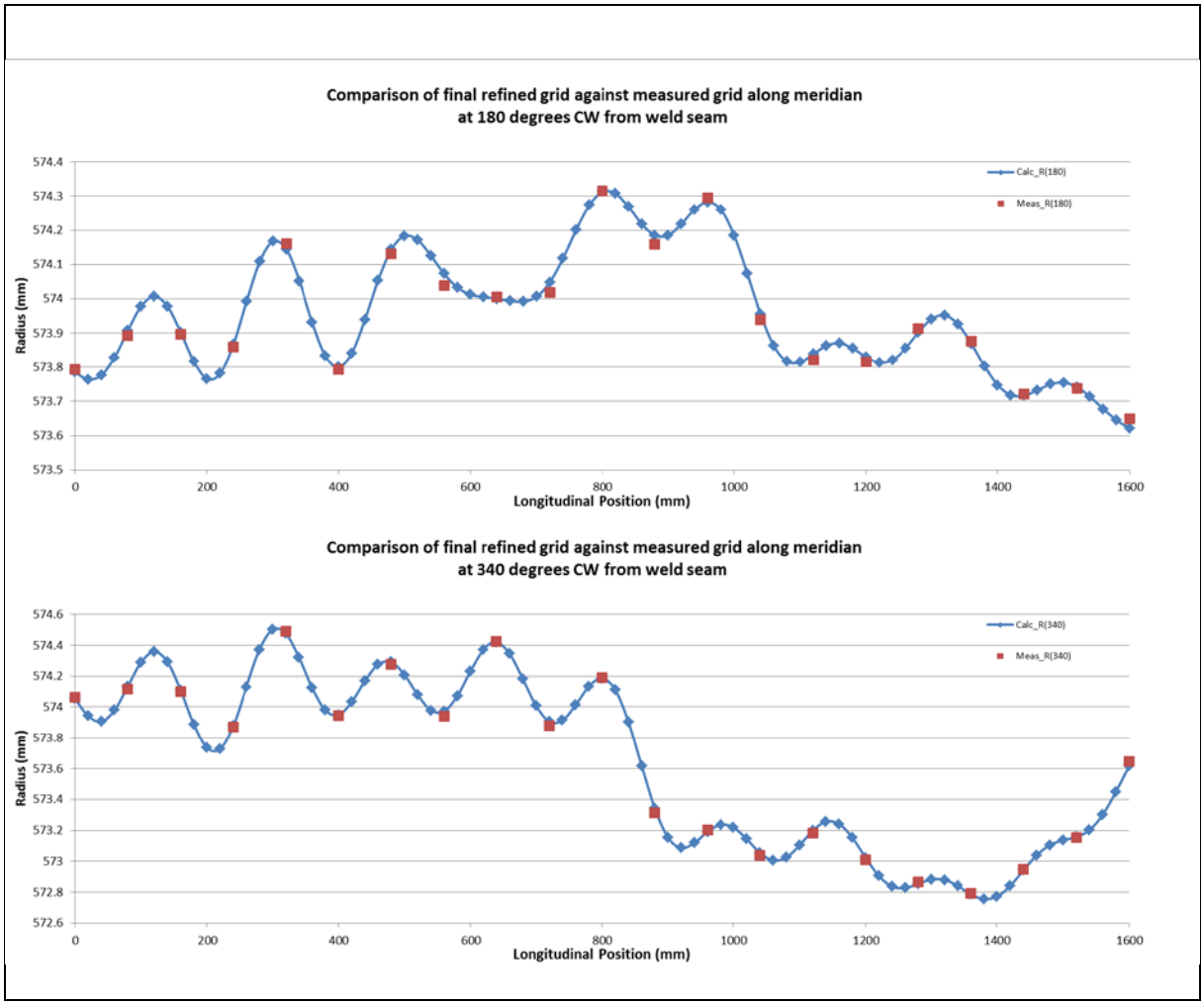

Figure 4. Comparison of measured and calculated radial values along two meridians. The range of radius axis values is restricted to exaggerate the variation from a mean radius of approximated 572 mm.

3.1.3 True centre position

As noted above, Equation (2) is modified from the original form given by Kendrick (1977) so that the true centre of each section is maintained at its correct position relative to the cylinder centreline axis. Figure 5 shows an example of the result that would occur if this were not done. The blue markers are the calculated radial values measured from the true centre (i.e. **n**=1 terms included in Equation (2) summation) and the green markers are the calculated radial values measured from the nominal centreline axis (**n**=1 term omitted). Due to the exaggerated scale, the variations between the two sets of values is clearly evident although the overall difference is actually relatively small in this case (0.32mm maximum), but this may not always be the case and so it is preferable to include the **n**=1 term in the Equation (2) summation.

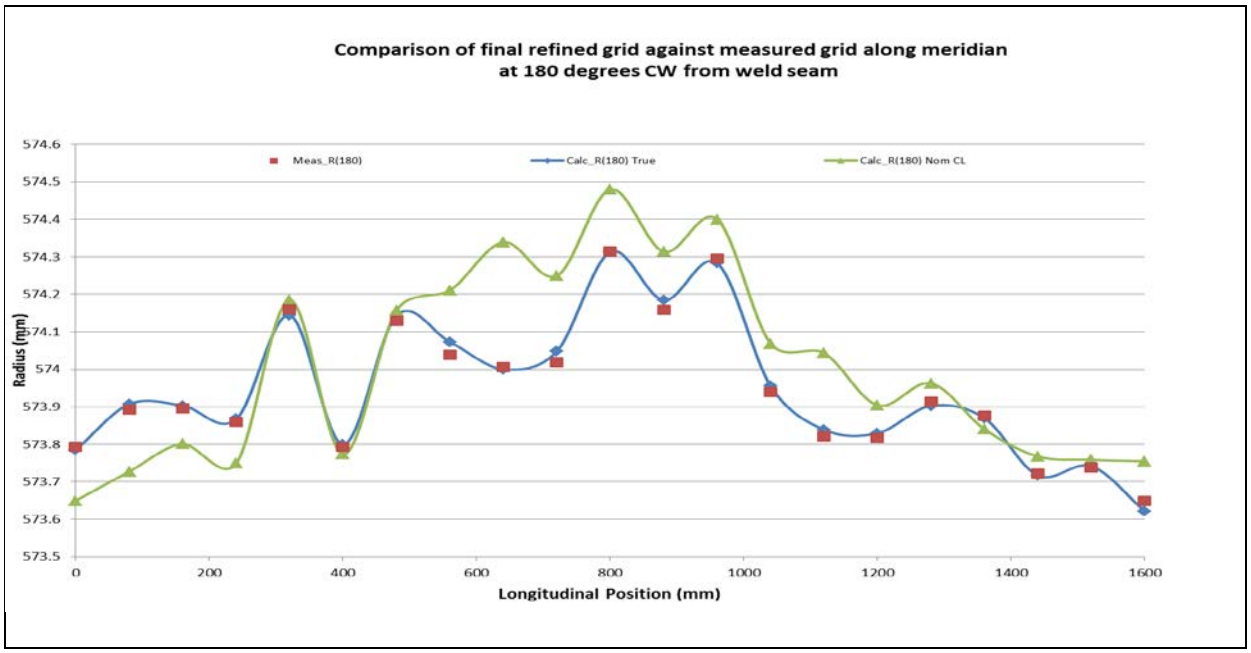

Figure 5. Comparison of measured and calculated radial values at 180 degree meridian. The blue line (diamond marker) has the centre of each section at the true centre whilst the green line (triangular marker) has the centre of each section on the nominal centreline axis. Radius axis values are restricted to exaggerate variation from mean.

4. Conclusions

It is important for NL FEA of pressure vessels that OOC deviations from a perfectly round shape and plate thickness variations can be accurately modelled so that reliable estimates of the collapse pressure may be obtained. As the measured values may be on a relatively coarse grid and not able to be applied directly to the refined grid FEM node and element definitions, suitable methods to interpolate from the measured values are needed. Proven methods that have wide general acceptance are Fourier series and bi-linear interpolation.

These methods have been implemented in an Excel spreadsheet to produce node and element data that can be used directly in Strand7 through the 'Online Editor' facility. Results from a test case show that accurate interpolation between measured data points is achieved.

5. Acknowledgements

Thanks is given to Defense Research and Development Canada who have kindly provided the test case measurement data used in this example and to Dr John MacKay for his helpful advice in relation to OOC mapping.

6. References

1. Kendrick, S.B. (1970), Externally pressurized vessels, in S.S. Gill (Ed.), The Stress Analysis of Pressure Vessels and Pressure Vessel Components, Pergamon Press, Toronto, pp.405–511, 1970.
2. Kendrick, S.B., (1977), Shape Imperfections in Cylinders and Spheres: Their Importance in Design and Methods of Measurement., IMechE Journal of Strain Analysis, Vol 12 No 2, 1977.
3. John R. MacKay, (2007), Structural Analysis and Design of Pressure Hulls: the State of the Art and Future Trends, Defence R&D Canada – Atlantic, Technical Memorandum DRDC Atlantic TM 2007-188, October 2007.

DEFENCE SCIENCE AND TECHNOLOGY GROUP DOCUMENT CONTROL DATA	1. DLM/CAVEAT (OF DOCUMENT)

2. TITLE	3. SECURITY CLASSIFICATION (FOR UNCLASSIFIED REPORTS THAT ARE LIMITED RELEASE USE (L) NEXT TO DOCUMENT CLASSIFICATION)
Refinement of Out of Circularity and Thickness Measurements of a Cylinder for Finite Element Analysis	Document (U) Title (U) Abstract (U)
4. AUTHOR(S) B.P. Phelps	5. CORPORATE AUTHOR Defence Science and Technology Group 506 Lorimer St Fishermans Bend Victoria 3207 Australia

6a. DST Group NUMBER	6b. AR NUMBER	6c. TYPE OF REPORT	7. DOCUMENT DATE
DST-Group-TN-1521	AR-016-603	Technical Note	September 2016

8. FILE NUMBER	9. TASK NUMBER	10. TASK SPONSOR	11. NO. OF PAGES	12. NO. OF REFERENCES
	07/386	CASG, HFSP	22	3

13. DST Publications Repository	14. RELEASE AUTHORITY
http://dspace.dsto.defence.gov.au/dspace/	Chief, Maritime Division

15. SECONDARY RELEASE STATEMENT OF THIS DOCUMENT

Approved for public release

OVERSEAS ENQUIRIES OUTSIDE STATED LIMITATIONS SHOULD BE REFERRED THROUGH DOCUMENT EXCHANGE, PO BOX 1500, EDINBURGH, SA 5111

16. DELIBERATE ANNOUNCEMENT

No Limitations

17. CITATION IN OTHER DOCUMENTS Yes

18. RESEARCH LIBRARY THESAURUS

Finite element analysis, Interpolation, Fourier analysis

19. ABSTRACT

The as-built out-of-circularity (OOC) deviations from a perfectly round shape and plate thickness variations of a cylinder that is subjected to external pressure are known to have a significant effect on the collapse strength and must be accurately represented in finite element analysis to obtain accurate results. Often it is necessary to interpolate measurements from a relatively coarse grid to a refined finite element model and methods that have wide general acceptance are Fourier series and bi-linear interpolation. These methods have been implemented in an Excel spreadsheet to produce node and element data that can be used directly in the Strand7 finite element package, but the methods employed are suitable for other software as well.